

Received March 31, 2018, accepted May 23, 2018, date of publication June 1, 2018, date of current version July 6, 2018.

Digital Object Identifier 10.1109/ACCESS.2018.2842721

# Compositional Structure Recognition of 3D Building Models Through Volumetric Analysis

XUAN SUN<sup>1,2</sup>, (Member, IEEE), QINGQUAN LI<sup>3</sup>, AND BISHENG YANG<sup>4</sup>

<sup>1</sup>Zhou Enlai School of Government, Nankai University, Tianjin 300350, China

<sup>2</sup>Experimental Teaching Center for Applied Social Science, Nankai University, Tianjin 300350, China

<sup>3</sup>Shenzhen Key Laboratory of Spatial Information Smart Sensing and Services, Shenzhen University, Shenzhen 518060, China

<sup>4</sup>State Key Laboratory of Information Engineering in Surveying, Mapping, and Remote Sensing, Wuhan University, Wuhan 430079, China

Corresponding author: Qingquan Li (liqq@szu.edu.cn)

This work was supported in part by the National Natural Science Foundation of China under Grant 41501427, in part by the Fundamental Research Funds for the Central Universities under Grant NKZXB1483, in part by the Project of the Asia Research Center, Nankai University, under Grant AS1522, and in part by the Open Research Fund Program of the Shenzhen Key Laboratory of Spatial Smart Sensing and Services.

**ABSTRACT** Structure is one of the most important properties of man-made objects, and it is beneficial for a number of applications. In this paper, we propose an effective method to recognize the 3-D building models' compositional structures, which represent the basic knowledge of human beings on the shape formation of the models in 3-D space. To overcome the shortcomings of the traditional algorithms that are focused on the detailed geometric features of the surface meshes, volumetric analysis is employed here to study the compositional structures of the building models from inside. To describe the general shape of a building model in 3-D space, the model is voxelized, and layered distance maps are generated to record its volumetric characteristics at different places. With reference to the value variation of the layered distance maps in the horizontal and vertical directions, different structural parts are identified in the voxel space, and the valid voxels are classified accordingly to obtain the voxel representation of each part. Based on the volume decomposition result, an extended topological graph is then constructed for description of the compositional structure of the building model. As the spatial relationships between different parts are analyzed from inside and the whole process is implemented in the voxel space, the method is immune to the complicated and confusing features on the surfaces of the building models, with the scale of the structure recognition determined by the discretizing resolution of the voxel space. In the experiments, three typical building models are chosen for discussion of the effectiveness and efficiency of the proposed approach, and some example applications are shown to demonstrate its potential usage in different fields.

**INDEX TERMS** Structure recognition, 3D building model, volumetric analysis, shape description.

## I. INTRODUCTION

With the development of computer graphics and mapping technology, 3D applications have been springing up these years, and 3D building models are playing a more and more important role in the applications of digital city and smart city. To satisfy the needs in practical applications, such as texture mapping [1], [2], efficient visualization [3]–[6] and semantic modeling [7], [8], much attention has been given to the treatments of the 3D building models in the latest decade. However, the data treatments are always not easy works, especially for the complex building models.

In order to ensure the correctness and quality of data treatment, it is necessary to take a preprocessing procedure to study some preliminary knowledge of the targeted models. Structure is just one of the most important properties of man-made objects [9]. In the applications of model generalization and simplification, some pioneering researches have been carried out to study the layouts of building models in the horizontal direction [10] and the geometric structures on the surfaces of building models [11], [12]. Whereas, there is very few works systematically discussing the 3D building models' compositional structures, which represent the basic

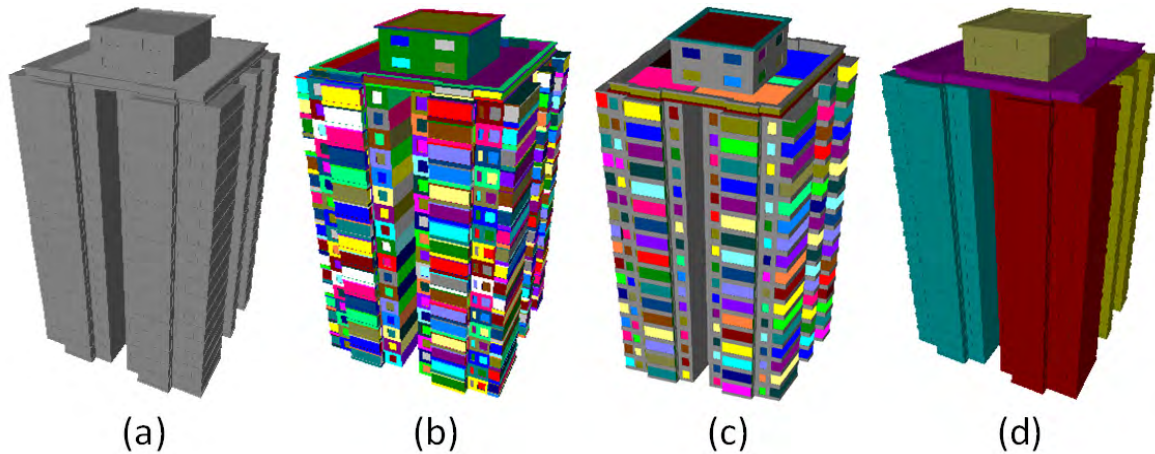


**FIGURE 1.** Structure recognition of a typical building model, with different parts rendered in different colors. (a) The original 3D model. (b) The recognition result obtained by the surface clustering algorithm. (c) The recognition result obtained by the geometric analysis algorithm. (d) The desirable compositional structure recognition result.

knowledge of human beings on the shape formation of the models in 3D space.

To recognize the compositional structures of 3D models, a number of algorithms have been proposed out for model segmentation and decomposition in the field of computer graphics [13]–[15]. Distinguished by the approaches used, the existing algorithms can be roughly classified into four categories: the surface clustering algorithms [16]–[18], the boundary detection algorithms [19], [20], the primitive fitting algorithms [21], [22], [23], and the algorithms based on geometric analysis [24]–[26]. Although the existing methods exhibit great capabilities in the processes of structure recognition of natural objects, they are not well suitable for the compositional structure recognition of building models (see Fig. 1).

The complex surfaces would fail most of the approaches to studying the shape formation of 3D building models from outside. First, the surfaces of building models always consist of both planar and irregularly curved patches, which makes it a complicated problem to design a flexible algorithm to detect all the partition edges with certain thresholds [27]. Second, the sharp details (e.g., windows, doors, carvings, ornaments) on the surfaces of 3D building models might be easily recognized as the boundaries of different structural parts and result in excessive decomposition [28]. Third, the non-manifold topologies (e.g., isolated points, edges, or facets) commonly seen in synthetic 3D building models might disorient the geometric treatments of the surface meshes and lead to incomplete or unreasonable decomposition results in the end [29]. Only if the volumetric characteristics are considered and the shapes of building models are studied from inside, all the problems stated above could be well solved.

In this paper, a novel method based on volumetric analysis is proposed to study the compositional structures of 3D building models. As the spatial relationships between different parts are analyzed from inside, the method is

immune to the complicated and confusing features on the surfaces of the building models (even suitable for surface models with broken topologies). The remaining parts of this paper are organized as follows. We give an introduction of the shape description scheme in the voxel space in Section II. In Section III, the process of volumetric analysis for structure recognition is elaborated in details. Section IV discusses the structure description of 3D building models. The experimental results and some example applications are presented in Section V. Finally, Section VI briefly concludes this paper.

## II. SHAPE DESCRIPTION IN THE VOXEL SPACE

Voxel representation is one of the most effective ways to describe the spatial occupation of any object in the 3D world [30]. Comparing with the traditional model that is constructed with triangular meshes, the voxel representation is able to give a more general view of the object's shape, without much information about the detailed features on the surface. For compositional structure recognition, it is proposed to make voxelization of the 3D building model firstly, and to study the characteristics of its shape in the voxel space.

### A. VOXELIZATION OF THE 3D BUILDING MODEL

In the process of voxelization, the 3D space is discretized with a specified interval (see Fig. 2b). Each voxel represents a regular spatial unit at a certain place in the discretized voxel space, and the voxel representation of any building model can be obtained through the procedure of voxel classification [31]. The main task is actually to distinguish the voxels inside and on the boundary of the building from the outside ones, with reference to the space occupation of the 3D model (see Fig. 2c).

All the existing approaches for voxelization are based on either slice cutting [32] or discrete sampling [33]. For simplicity, discrete sampling algorithm is employed here to

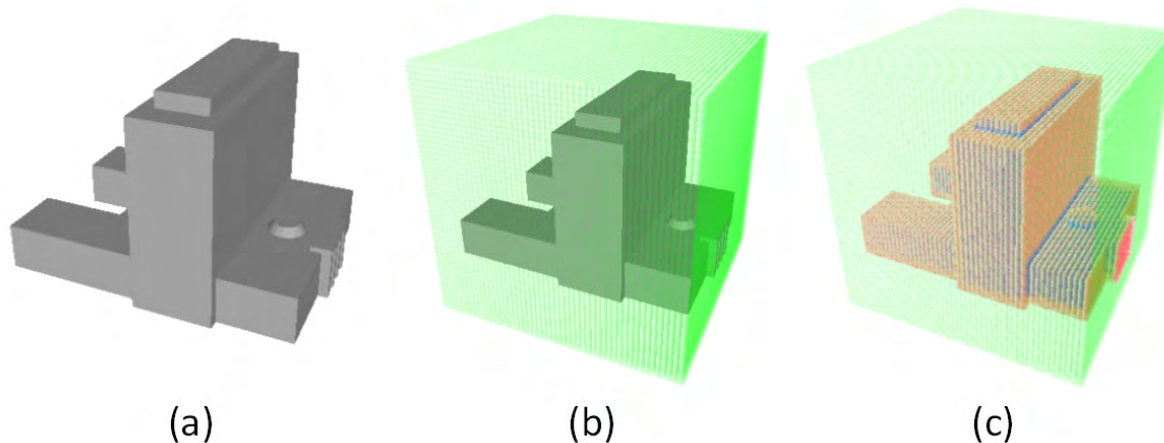


**FIGURE 2.** Voxelization of the 3D building model. (a) The original building model. (b) The voxel space obtained through space discretization with a specified interval. (c) The representation of the building model in the voxel space, where the boundary voxels are the red ones and inner voxels are blue.

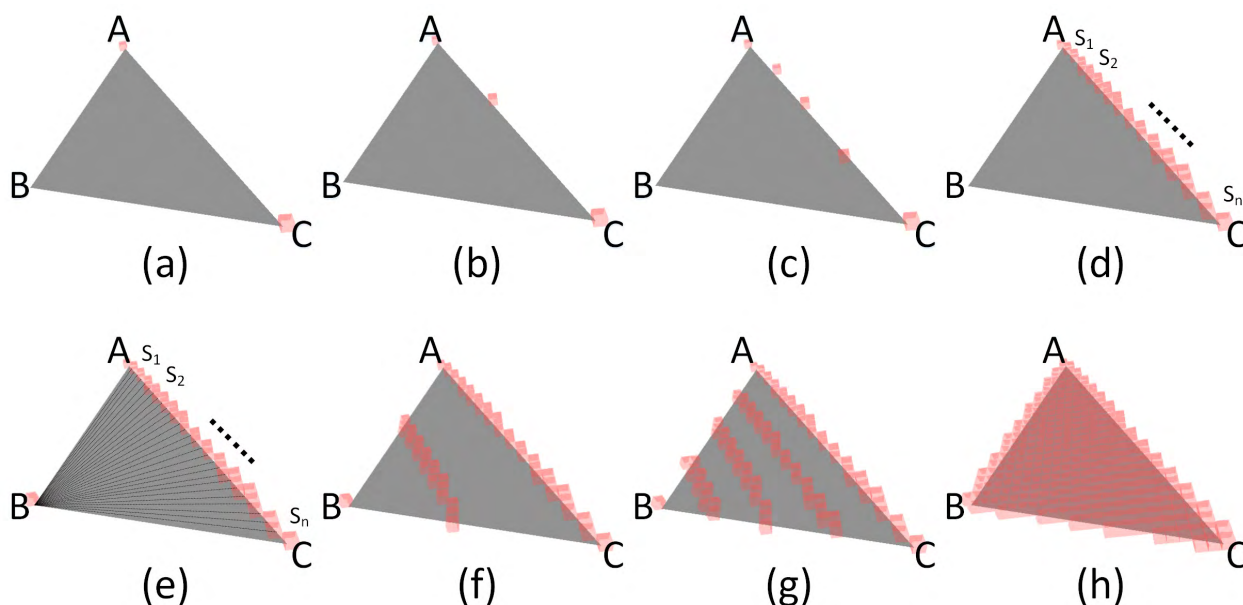


**FIGURE 3.** Voxelization of a triangular facet based on point sampling algorithm. (a) – (d) Point sampling along the edge of AC with a successive dichotomy method. (e) – (h) Point sampling along each of the lines connecting endpoint B and the sample points obtained along AC.

determine the exact location of each part of its surfaces in the voxel space (see Fig. 3). However, to ensure the completeness of the result and the efficiency of the algorithm, the sample points are chosen with a successive dichotomy method in each triangular facet, where new points will be selected at middle of the existing neighboring sample points to enhance the sampling density of the surface. The voxels that spatially contain the sample points will be identified as boundary voxels, and the iteration of point sampling would not be stopped until no more new boundary voxel can be found. Given a triangular facet  $ABC$ , the three endpoints are taken as the initial sample points, and it is proposed to increase the sample density with two steps. First, the longest edge

(e.g. AC in Fig. 3) is taken as the basic sampling line, and a number of sample points are selected (e.g. A,  $S_1$ ,  $S_2$ , ...,  $S_n$ , C in Fig. 3d) with the successive dichotomy method to ascertain the valid voxel representation of the edge (the common edges of neighboring facets might be sampled two times). Second, based on the sample points on the longest edge and another endpoint of the facet (e.g. B in Fig. 3), a number of new sampling lines are generated (e.g. BA,  $BS_1$ ,  $BS_2$ , ...,  $BS_n$ , BC in Fig. 3e), and within the new sampling lines all the other sample points of the facet are able to be determined.

For identification of the inner voxels, traversing test is carried out to make clear the spatial relationship of each

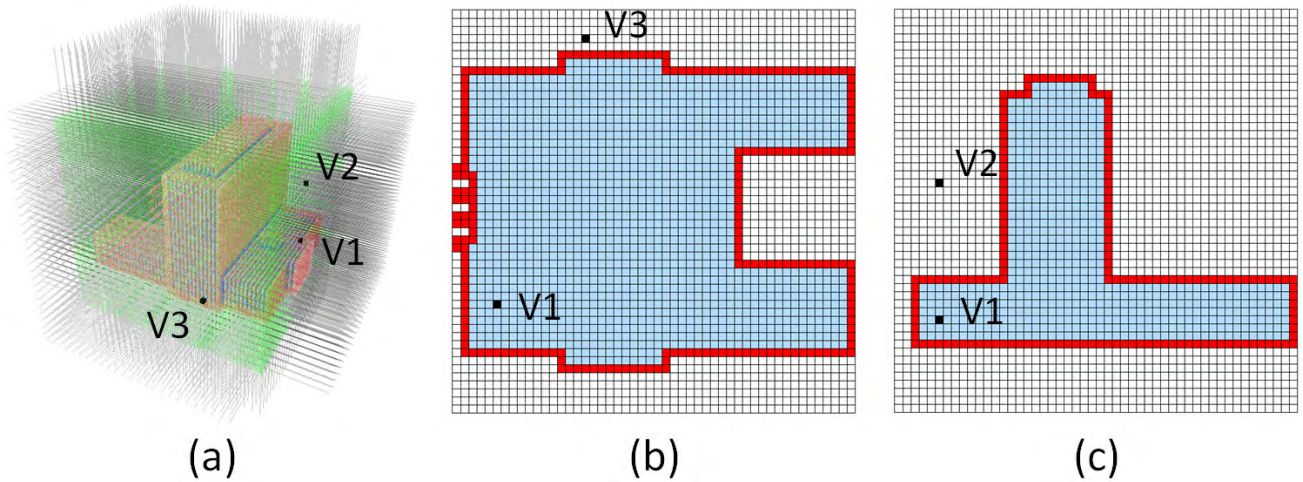


**FIGURE 4.** The process of inner voxel identification. (a) Illustration of the traversing test carried out with testing rays from different directions. (b) The top view of certain vertical section of the voxel space that contains  $V_1$  and  $V_3$ . (c) The left view of certain side section of the voxel space that contains  $V_1$  and  $V_2$ .

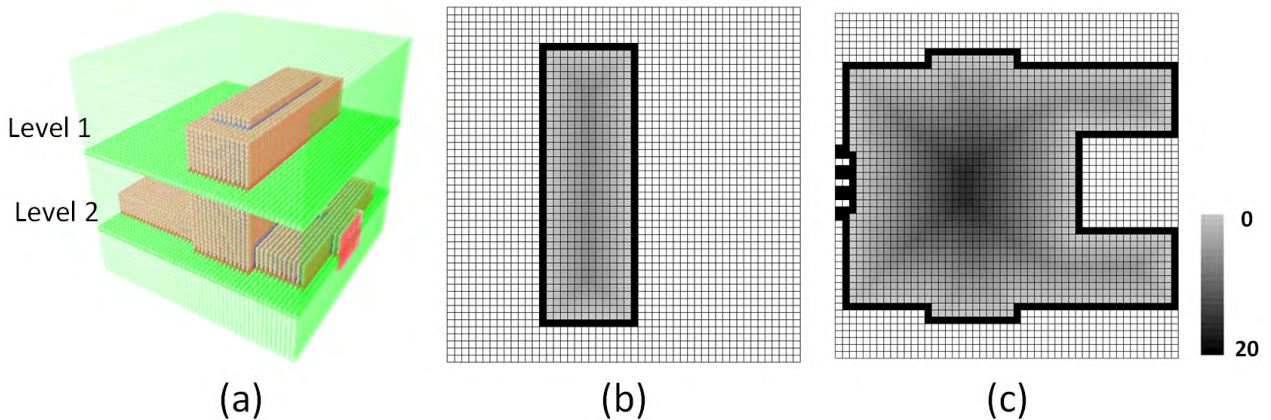


**FIGURE 5.** Generation of layered distance maps for a building model. (a) Illustration of the layered structure of the distance maps in the voxel space (e.g. level 1 and level 2). (b) The distance map for the voxels in level 1. (c) The distance map for the voxels in level 2.

voxel and the building model (see Fig. 4). In the 3D space, a number of testing rays are emitted from different directions (for simplicity, the testing rays parallel to the axes are chosen in the implementation). With reference to the boundary voxels that are obtained in the previous procedure, it is possible to figure out the relative positions of the other voxels according to the traversing states of the testing rays that pass through each of them in the extending process. Considering the complicated structures of building models (e.g. the backyards or activity spaces on the lower floor) and the possible errors of boundary voxel identification in the previous step due to unrestricted modeling processes (e.g. surfaces inside building models), the traversing states of different testing rays are cross validated for precise judgment. If all the testing rays have traversed some boundary voxels before reaching the voxel to test, the voxel will be labeled as an inner voxel (e.g.  $V_1$  in Fig. 4); otherwise, it is

outside the boundary of the building model (e.g.  $V_2$ ,  $V_3$  in Fig. 4).

### B. LAYERED DISTANCE MAP GENERATION

The Euclidean distance map inside the 3D model can well reflect the volumetric characteristics of the corresponding object [34], [35]. With consideration of the floor-by-floor architecture of buildings in the real world, it is proposed to calculate the distance parameters in each vertical level of the voxels independently and generate layered distance maps for shape description of the building model in the voxel space (see Fig. 5).

In this paper, we take the Euclidean distance of each inner voxel to the nearest boundary voxels in the same level as the basic parameter and accurately calculate it with a mathematical way. Assume  $V_{i,l}$  is an inner voxel at level  $l$ ,  $V_{o,l}$  is a boundary voxel in the same level, and

$(X_{i,l}, Y_{i,l}), (X_{o,l}, Y_{o,l})$  are the discrete horizontal coordinates of  $V_{i,l}$  and  $V_{o,l}$ , the distance parameter  $DVal(V_{i,l})$  of  $V_{i,l}$  can be calculated according to the following formula.

$$D(V_{i,l}, V_{o,l}) = \sqrt{(X_{i,l} - X_{o,l})^2 + (Y_{i,l} - Y_{o,l})^2}$$

$$DVal(V_{i,l}) = \min_o(D(V_{i,l}, V_{o,l})) \quad (1)$$

One building model can have different versions of layered distance maps, which represent the volumetric characteristics of the model at different scales. The higher the resolution of the voxel space is, the more small parts could be reflected in the layered distance map. In order to describe the shape variation of the main body and intentionally hide the uninterested small compositional parts of the building model, it is important to choose proper discretizing interval of the space in the process of voxelization. The “scale effect” of the discretizing resolution is further discussed in the section of experiments and applications, and the key consideration is the granularity of the structure recognition.

### III. VOLUMETRIC ANALYSIS AND STRUCTURE RECOGNITION

With the aid of the layered distance maps, the shape of the building model is able to be analyzed for recognition of different structural parts in the voxel space. The mid-voxels are the local kernels of the building model at different places. To reduce the dimensionality of the volumetric analysis, the mid-voxels are extracted in each vertical level of the voxel space firstly as the shape representatives of the building model. Then, the main structural parts are identified by means of mid-voxel clustering in both horizontal and vertical directions. Finally, all the other valid voxels are classified according to the clustering result of the mid-voxels to figure out the exact space formation of each structural part.

#### A. MID-VOXEL EXTRACTION

As the parameter value of the layered distance map is smaller near the boundary and bigger in the middle of the model, mid-voxels are extracted at different vertical levels of the voxel space by means of local maximum seeking (see Fig. 6a). In order to avoid the morphological noises caused by the voxelization, two-order maximum judgment is adopted in the process of mid-voxel extraction, where the parameter value of each voxel in the corresponding layered distance map is compared with that of the neighboring voxels to search for the ones with the maximum distance parameters within the  $5 \times 5$  window. If no value is bigger than that in the middle of the searching window, the targeted voxel is labeled as a mid-voxel

Due to the complex structures of buildings, there might be a number of mid-voxels  $M_l = \{m_{1,l}, m_{2,l}, m_{3,l}, \dots, m_{n,l}\}$  scattered in a certain vertical level  $l$  of the voxel space. Taking the distance parameter  $DVal(m_{i,l})$  of the mid-voxel  $m_{i,l}$  as the radius, the circular range  $C_{i,l}$  centered at  $m_{i,l}$  is actually the maximum open space inside the building model locally, reflecting the volumetric size of the model at the

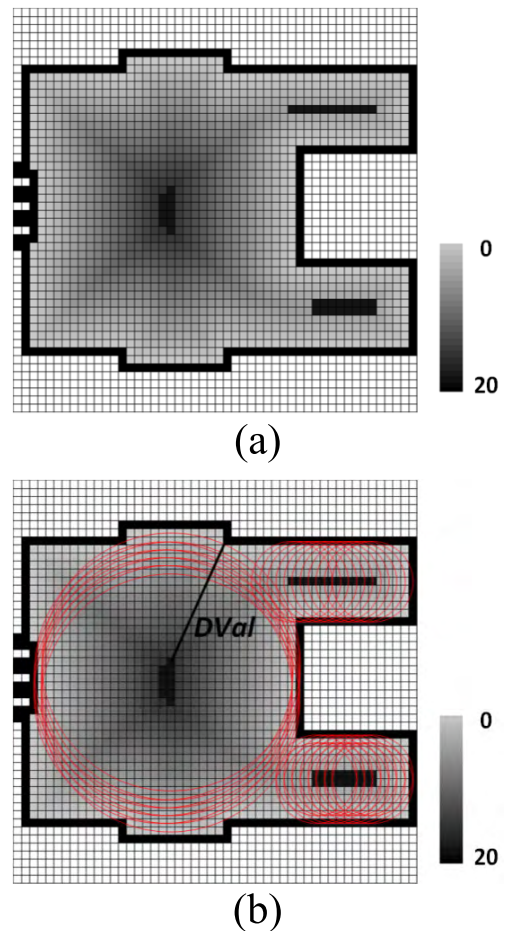


**FIGURE 6.** Mid-voxel extraction and  $DVal$  parameters of the mid-voxels in certain vertical level of the voxel space. (a) The result of mid-voxel extraction. (b) Illustration of the  $DVal$  parameter calculation.

specific place (see Fig. 6b). As the core parameter of the layered distance map,  $DVal$  is also considered as an important clue for volumetric analysis.

#### B. STRUCTURAL PART IDENTIFICATION

Shape continuity is the basic characteristic of each structural part. The volumetric spaces belonging to the same structural part not only need to be spatially adjacent but also should have similar size in geometry. To identify all the structural parts  $P = \{p_1, p_2, p_3, \dots, p_k\}$  of the building model, the mid-voxels extracted at different levels of the voxel space have to be clustered in both horizontal and vertical directions. In the horizontal direction, each structural part can be represented by several neighboring mid-voxels with similar  $DVal$  value (see Fig. 7a), for example,  $p_r$  is able to be represented by  $v$  mid-voxels  $Rep(p_{r,l}) = \{m_{a,l}, m_{a+1,l}, \dots, m_{a+v,l}\}$  in level  $l$ . In the vertical direction, the clusters showing consistent variation of size at neighboring levels of the voxel space can be merged together to obtain the complete representation of the structural part (see Fig. 7b), for example,  $p_r$  could be represented by  $w$  mid-voxel clusters  $Rep(p_r) = \{Rep(p_r, b), Rep(p_r, b+1), \dots, Rep(p_r, b+w)\}$  in different levels.

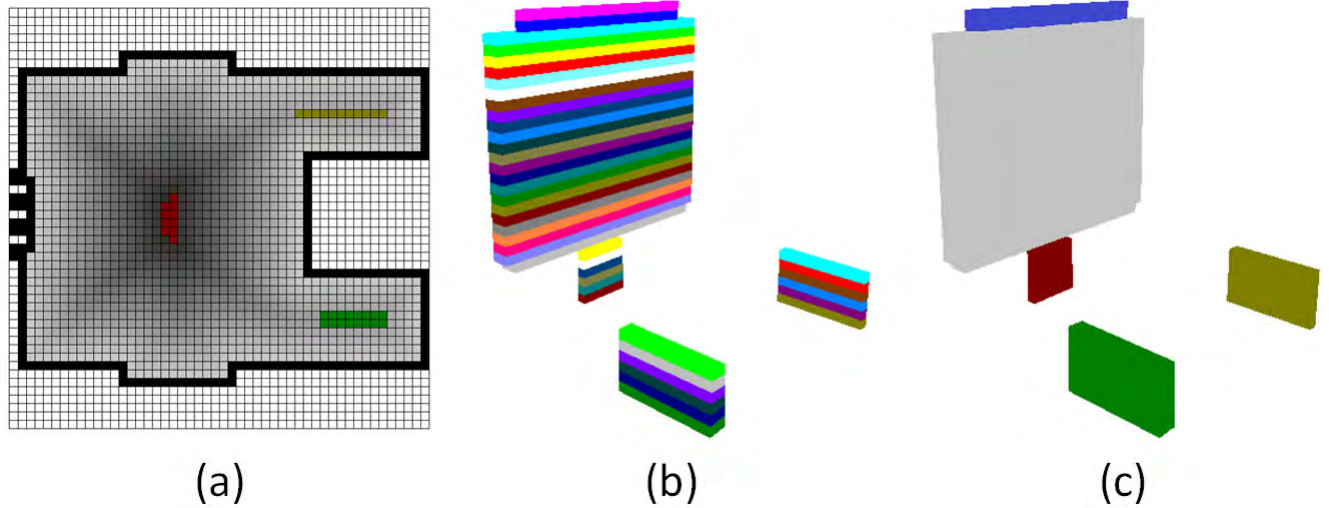


**FIGURE 7.** Structural part identification by means of mid-voxel clustering. (a) Mid-voxel clustering in the horizontal direction. (b) Mid-voxel clusters obtained in different vertical levels of the voxel space. (c) Mid-voxel cluster merging in the vertical direction.

## 1) MID-VOXEL CLUSTERING IN THE HORIZONTAL DIRECTION

Since the voxelization direction might not fit well with the layout of the building model, there are always gaps between the mid-voxels that actually belong to the same structural part in the horizontal direction. To avoid misleading clustering results, it is proposed to relax the clustering rule and allow the mid-voxels that are not strictly neighboring to each other to be clustered together. Thus, there are two thresholds for the mid-voxel clustering in the horizontal direction. One is the shape threshold  $T_s$ , which is used for judgment of whether the local spaces that the mid-voxels represent have the similar size; and the other is the neighborhood threshold  $T_n$ , which is used to decide whether the mid-voxels can be regarded as neighboring in space or not. To ensure the shape consistency of each structural part,  $T_s$  is always set as 1 or 2 for comparison of the distance parameters of the mid-voxels to be clustered, e.g.  $\{DVal(m_{i,l}), DVal(m_{j,l})\}$ . As to  $T_n$ , it is preferred to adopt the minimum distance radius parameter  $Min(DVal(m_{i,l}), DVal(m_{j,l}))$  as the allowed maximum gap  $|m_{i,l}m_{j,l}|$  between the two mid-voxels. Based on all the above rules, the clustering process of mid-voxels in the horizontal direction can be formulated as a region-growth process (see **Algorithm 1**).

## 2) CLUSTER MERGING IN THE VERTICAL DIRECTION

In the vertical direction, some aggregate parameters of the mid-voxel clusters are taken as the references for judgment of shape continuity (see **Fig. 8**). On one hand, the positions of the barycenters of the mid-voxel clusters obtained respectively at different levels of the voxel space are compared to decide which ones are vertically aligned; on the other hand, the  $DVal$  parameters of the aligned mid-voxels clusters are analyzed to determine the size variation pattern of the building model at the specific parts.

## Algorithm 1 Mid-Voxels Clustering in the Horizontal Direction

---

```

1: input:  $M_l = \{m_{1,l}, m_{2,l}, m_{3,l}, \dots, m_{n,l}\}$ 
2:  $P_l \leftarrow \Phi$ 
3: for each  $m_{i,l}$  in  $M_l$ 
4:   unmark  $m_{i,l}$ 
5:    $t \leftarrow 1$ 
6:   for  $i \leftarrow 0$  to  $n$ 
7:     if  $m_{i,l}$  is unmarked
8:       mark  $m_{i,l}$ 
9:        $Rep(p_{t,l}) \leftarrow \{m_{i,l}\}$ 
10:       $p_{t,l} \leftarrow \text{RGrowth}(m_{i,l}, p_{t,l})$ 
11:       $P_l \leftarrow P_l \cup \{p_{t,l}\}$ 
12:       $t \leftarrow t + 1$ 
13: output:  $P_l$ 
end procedure
function  $\text{RGrowth}(m_{i,l}, p_{t,l})$ 
  for each  $m_{j,l}$  ( $i \neq j$ ) in  $M_l$ 
  if  $m_{j,l}$  is unmarked
  if  $|m_{i,l}m_{j,l}| \leq T_n$  and  $-T_s \leq DVal(m_{i,l}) - DVal(m_{j,l}) \leq T_s$ 
  mark  $m_{j,l}$ 
   $Rep(p_{t,l}) \leftarrow Rep(p_{t,l}) \cup \{m_{j,l}\}$ 
   $p_t \leftarrow \text{RGrowth}(m_{j,l}, p_{t,l})$ 
return  $p_{t,l}$ 
end function

```

---

Due to the decorative features on the surfaces and some artistic architectures (e.g. the diagonal body), the barycenters of the mid-voxel clusters belonging to the same structural part might not be strictly aligned in the vertical direction, and a tolerance of small horizontal offset need to be considered in the process of continuous shape searching. For the balance of effectiveness and correctness, a two-voxel-unit

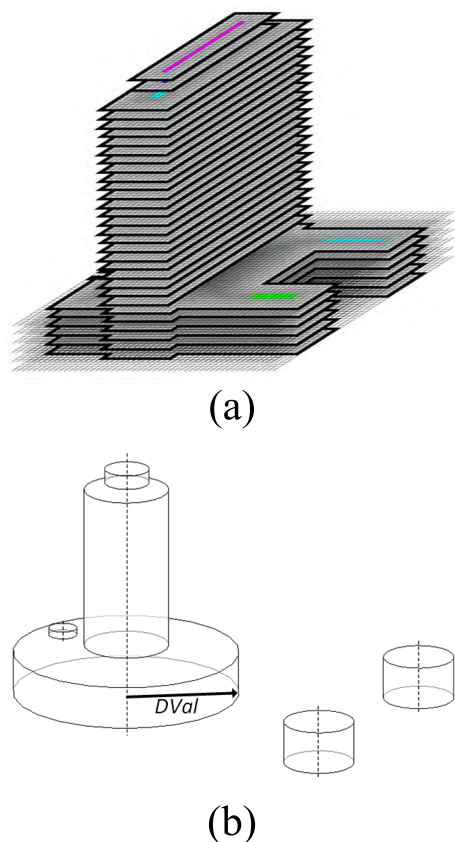


**FIGURE 8.** Cluster merging in the vertical direction. (a) The mid-voxel clusters obtained respectively in different levels of the voxel space. (b) Shape continuity judgment based on the positions of the mid-voxel clusters' barycenters and the variation of average *DVal* parameters.

offset is allowed in the practice of the position comparison of the barycenters in the neighboring levels of the voxel space.

As to the *DVal* parameter analysis, the architectural style of the building model is the key point for consideration. To fit in with the basic recognition tendencies of human beings on the continuous and convex shapes [36], four common-seen types of continuity are taken into account.

*a: CONSISTENTLY SHAPED*

The structural part is consistently shaped at different heights in the vertical direction. Almost all styles of building models have some structural parts of this type, such as the common-seen storey architecture of the building models (see Fig. 9a for example).

*b: PROGRESSIVELY SHRINKING*

The structural part is progressively shrinking from bottom to top in the vertical direction. The roofs of building models are very likely to represent this type of shape continuity in geometry, especially the ones of the church or tower models (see Fig. 9b for example).

*c: PROGRESSIVELY SWELLING*

The structural part is progressively swelling from bottom to top in the vertical direction. Although this type of shape continuity is very rare in the building models due to the limitation of architectural mechanics, it might exit in some artistic building models (see Fig. 9c for example).

*d: SPINDLE SHAPED*

This type of shape continuity is a combination of type 2 and 3, where the structural part is progressively swelling and then progressively shrinking from bottom to top in the vertical direction. In byzantine architectures, lots of structural parts are spindle shaped (see Fig. 9d for example).

**C. VOLUME DECOMPOSITION**

The core task of volume decomposition is to assign all the valid voxels of the building model into specific structural parts represented by the clustered mid-voxels. For determination of the structural part that each voxel belongs to, the attraction forces (*AF*) from different mid-voxels are calculated and compared for evidence of voxel classification. To obtain the accurate voxel representation of each structural part, the classification result is further modified to fit in with the various shape of the building model by means of separating edge adjustment.

1) VOXEL CLASSIFICATION WITH *AF* PARAMETER

With consideration of the spatial proximity and the various sizes of the structural parts, the *AF* parameter are mainly related with two factors, the distance between the mid-voxel and the targeted voxel and the *DVal* parameter of the mid-voxel. As to the former factor, it is obvious that the closer the two voxels are, the more likely they belong to the same part. For the latter one, which is able to reflect the maximum covering range of the structural part at certain place, the bigger the mid-voxel's *DVal* parameter is, the bigger possibility that the corresponding structural part covers the targeted voxel in the horizontal direction. With reference to the classic gravity model, the parameter  $AF(V_{mid}, V_0)$  from certain mid-voxel  $V_{mid}$  to any voxel  $V_0$  in the same level can be calculated with following formula, where  $DSqr(V_{mid}, V_0)$  stands for the squared distance between  $V_{mid}$  and  $V_0$ .

$$AF(V_{mid}, V_0) = DVal(V_{mid}) / DSqr(V_{mid}, V_0) \quad (2)$$

By comparison of the *AF* parameters from all the mid-voxels in the same vertical level of the voxel space, the valid voxels can be classified into different categories which represent the spatial formation of the structural parts. As the shape of the building model is not fully considered in the process of voxel classification, there are always vague separating edges between different structural parts in the same level (see Fig. 10).

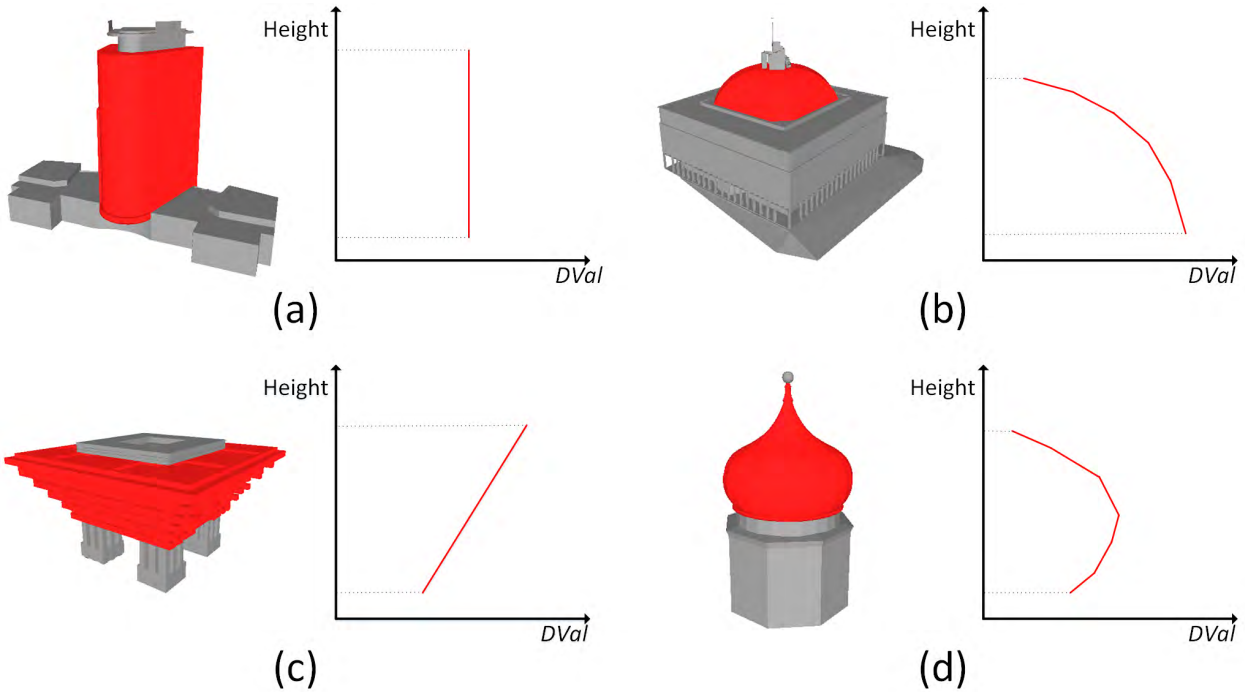


**FIGURE 9.** The four types of shape continuity of the building model's structural parts in the vertical direction (the red is the parts of concerns). (a) An example of the consistently shaped part in a building model. (b) An example of the progressively shrinking part in a building model. (c) An example of the progressively swelling part in a building model. (d) An example of the spindle shaped part in a building model.

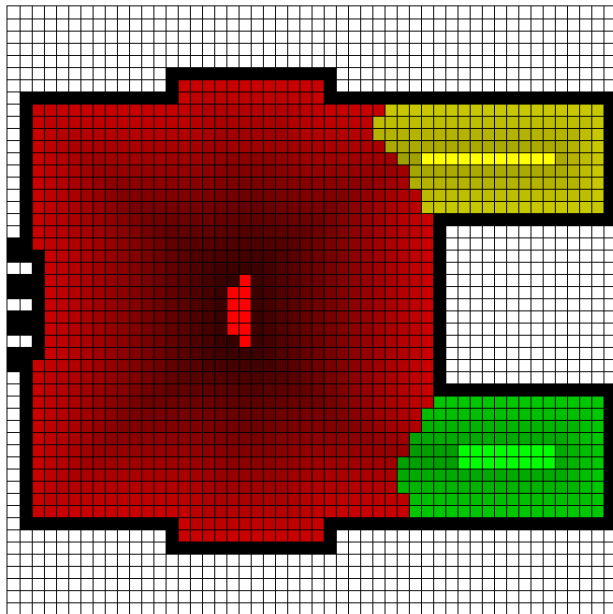


**FIGURE 10.** The voxel classification result in certain vertical level of the voxel space (the mid-voxels are the gray ones, and the valid voxels belonging to different structural parts are rendered in various colors).

## 2) SEPARATING EDGE ADJUSTMENT

The cuts that minimizes the interface between different parts are always recognized as the optimal separating edges [37]. For correction of the volume decomposition result, it is

proposed to search along the boundary of the building model and make adjustments to the existing separating edges based on the minimal rule. First, to figure out the original separating edges, the voxels lying between each two different structural parts in the same level of the voxel space are identified through neighborhood judgment and connected from head to tail. Second, the straight-line segment between the two endpoints of each separating edge is taken as the initial optimized edge, which makes the interface between the different parts smaller. Third, the positions of the two endpoints of the optimized edge are adjusted iteratively until the length of the new edge turns to be the shortest. In the process of the iterative adjustment, only the boundary voxels in the neighborhood of the endpoints are tested. If the separating edge's length gets shorter after adjustment, we take the tested boundary voxel as the new endpoint; otherwise, we keep the endpoint where it was. The two endpoints of each separating edge are adjusted alternately and independently. Since the original separating edges obtained through voxel classification are always nearly correct, it won't take a long time to achieve the optimal ones. Finally, we re-cluster all the valid voxels of the building model to fit in with the optimal separating edges obtained in each level (see Fig. 11).

Integrating the modified voxel classification results in different vertical levels, the building model is able to be decomposed into a number of structural parts in the voxel space, where the spatial extent of each part is clearly outlined (see Fig. 12).



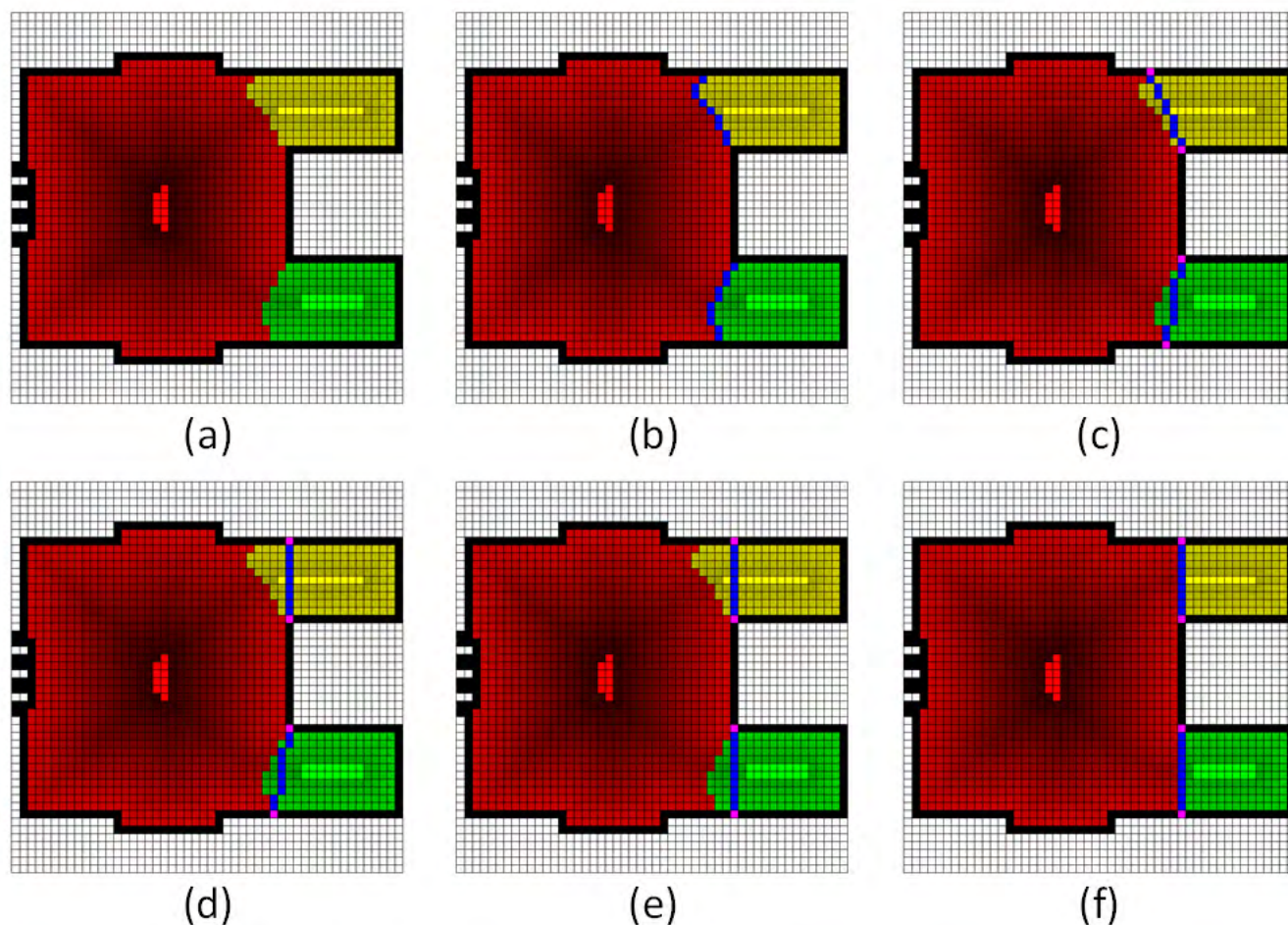


**FIGURE 11.** Separating edge adjustment in certain vertical level of the voxel space. (a) The original classification result of the valid voxels. (b) Identification of the original separating edges (blue lines). (c) Detection of the straight-line segment between the endpoints (red points) of the original separating edges. (d)-(e) adjustments of different separating edges. (f) The modified voxel classification result.

**IV. STRUCTURE DESCRIPTION WITH EXTENDED TOPOLOGICAL GRAPH**

Based on the volume decomposition result, an extended topological graph (ETG) is constructed for description of the compositional structure of the building model. In the ETG, each structural part is degenerated to a node, and the connection relationship of every two neighboring parts is represented by an arc that connects the corresponding nodes (see Fig. 13 for example). For better illustration of the spatial composition of the building model, the volume of each structural part is implied by the size of the node, and the relative positions of different parts are depicted with the directions of the arcs. The size parameter of each node in ETG can be roughly calculated by multiplying the number of the classified voxels belonging to the same part with the volumetric size of the voxel unit. The direction of each arc is calculated based on the coordinate difference of the two neighboring parts' central points in the voxel space.

Aside from the spatial construction, geometric attributes are also important to structure description of complex models [38]. For 3D building models, some properties of the structural parts and supplementary explanation about the connection relationships are recorded as the attributes of nodes and arcs in the ETG. As to the nodes, the approximate height, the extension direction, major-minor axis ratio of the structural parts in the horizontal direction and the type of continuity represented in the vertical direction are all meaningful attributes that can be obtained from the volumetric representations in the voxel space. As to the arcs, one of the most significant information is whether the neighboring parts are connected to each other side by side in the horizontal direction or level by level in the vertical direction.

Thus, the ETG of the 3D building model can be conceptually expressed as  $G = \{V, E, A_v, A_e\}$ , where  $V$  stands for the collection of nodes,  $E$  stands for the collection of arcs,  $A_v$  stands for the collection of attributes of nodes, and  $A_e$  stands for the collection of attributes of arcs.

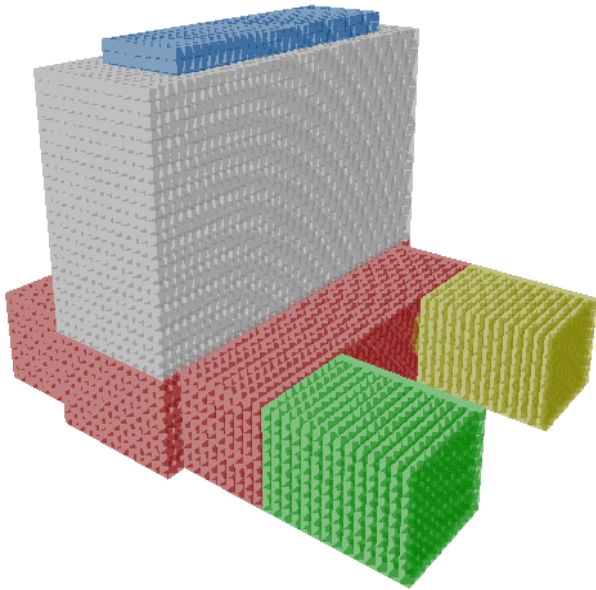


**FIGURE 12.** The volume decomposition result of the building model in the voxel space.

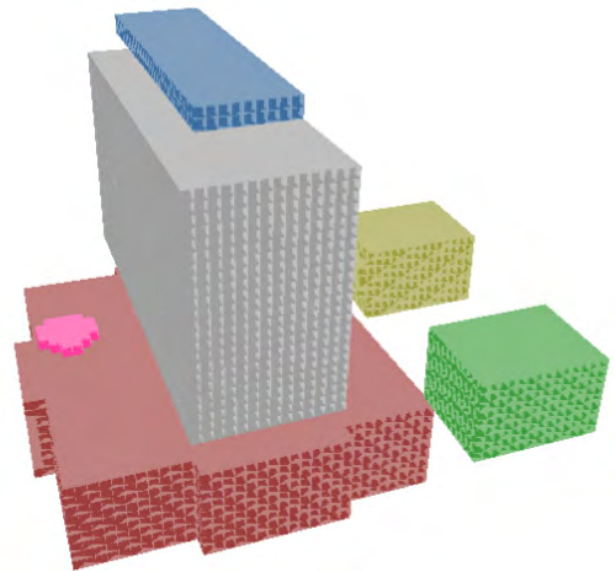
## V. EXPERIMENTS AND APPLICATIONS

For demonstration of the capability and wide usage of the proposed structure recognition method, experimental results on typical building models and extensive discussions about the potential applications are given in the following paragraphs.

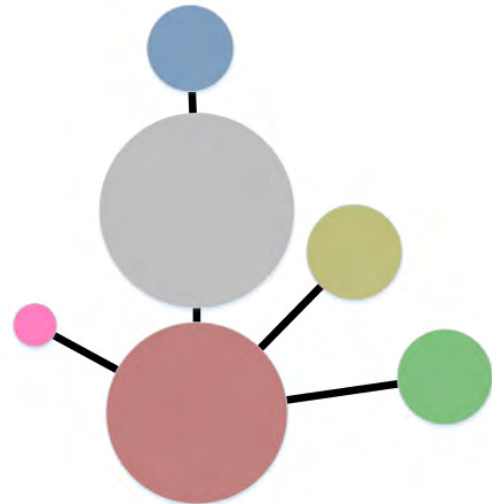
### A. EXPERIMENTS ON TYPICAL BUILDING MODELS

We conducted experiments on a wide range of building models, including the surface models constructed with classic meshing algorithms and the synthetic models constructed with commercial modeling softwares. To verify the effectiveness of the approach, three typical building models were selected for discussion (see Fig. 14). The first one is a model of a European museum that has a complicated structure in the horizontal direction; the second is a model of the typical Asian tower which represents a complex structure in the vertical direction; and the third model is a modern building that is composed of several parts in both horizontal and vertical directions.

With consideration of the scale effect in shape description and the size difference of the building models, we took both 1/30 and 1/50 of the maximum dimension of each model as the discretizing resolutions of the voxel space and conducted comparative experiments for test. From the experimental results, we can see that various types of compositional parts of the building models were recognized, with detailed parts merged under the coarser discretizing resolution and separated apart under the finer resolution. For the European museum (see Fig. 14a), all the hub spaces (e.g. the lobbies) were successfully recognized when the unit-to-whole resolution (UWR) of the voxel space was 1/30, and



(a)



(b)

**FIGURE 13.** Construction of the ETG for a building model. (a) The volumetric representations of different structural parts of the building model. (b) The ETG constructed based on the volume decomposition result.

all the linking spaces (e.g. the corridors) between the hubs were obtained when the UWR was 1/50. For the Asian tower (see Fig. 14b), different stories of the model were distinguished under 1/30 UWR, and the relationships between the roofs and the functional spaces could not be recognized unless the UWR is raised to 1/50. As to the modern building complex (see Fig. 14c), all the small extruding parts and narrow gaps between different parts were neglected under 1/30 UWR but effectively recognized out when the voxel size was raised up.

Judging from the statistics in Tab. 1, the procedure of voxelization was the main source of the noises

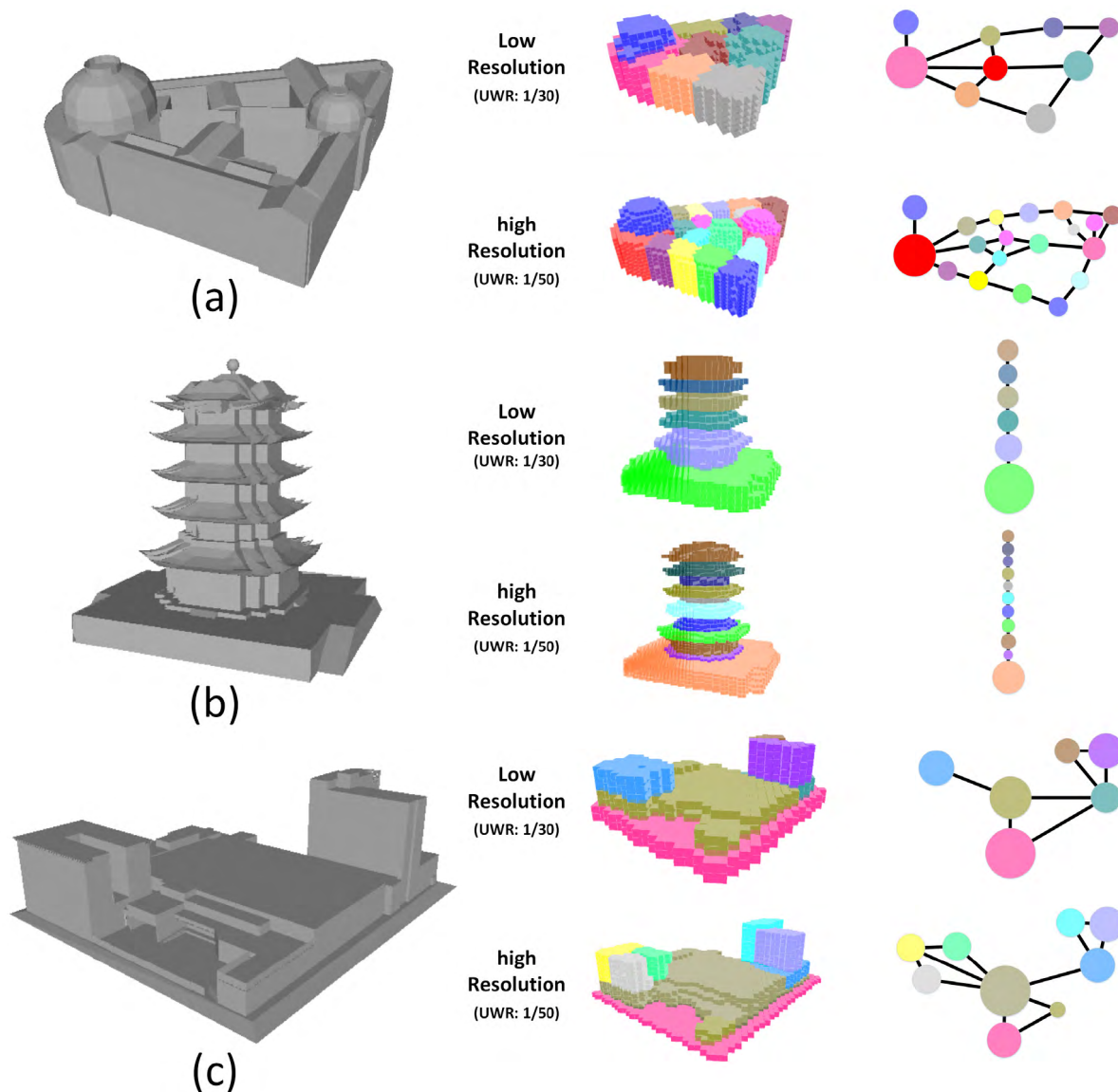


**FIGURE 14.** Compositional structure recognition of different styles of building models. (a) Building model of a European museum. (b) Building model of an Asian tower. (c) Building model of a modern building.

**TABLE 1.** Statistics of the structure recognition results of the example models in the voxel space.

| Model           | Resolution |                              | Sum Volume  |                        | Minimum volume |                        |
|-----------------|------------|------------------------------|-------------|------------------------|----------------|------------------------|
|                 | UWR        | Voxel size (m <sup>3</sup> ) | Voxel count | Size (m <sup>3</sup> ) | Voxel count    | Size (m <sup>3</sup> ) |
| European museum | 1/30       | 62.08                        | 2385        | 148060.80              | 164            | 10181.12               |
|                 | 1/50       | 12.80                        | 9886        | 126540.80              | 356            | 4556.8                 |
| Asian tower     | 1/30       | 8.37                         | 4476        | 37464.12               | 299            | 2502.63                |
|                 | 1/50       | 1.73                         | 17035       | 29470.55               | 343            | 593.39                 |
| Modern building | 1/30       | 36.26                        | 1879        | 68132.54               | 42             | 1522.92                |
|                 | 1/50       | 7.53                         | 6021        | 45338.13               | 38             | 286.14                 |

Resolution is depicted by the parameters of the unit-to-whole resolution (UWR) and the geometric size of the voxel unit at the same time. Sum volume stands for the volume of the building model, and Minimum volume is the volume of the structural part with the minimum size, both reflected by the parameters of the voxel count and the geometric size.

and deviations. Due to the fuzziness of the space occupation of the boundary voxels, the volumes of the building models could be blown up to some extent under coarse discretizing

resolution, producing additional bumps and filling up small pits on the surfaces. The more complicated surface the model had, the greater fuzziness of shape description there was

TABLE 2. Execution statistics of the structure recognition method on the example models.

| Model           | Complexity | UWR  | Model voxelization | Time (milliseconds)            |                      |       | Result |  |
|-----------------|------------|------|--------------------|--------------------------------|----------------------|-------|--------|--|
|                 |            |      |                    | Structural part identification | Volume decomposition | Nodes | Arcs   |  |
| European museum | 696        | 1/30 | 31                 | 63                             | 31                   | 9     | 10     |  |
|                 |            | 1/50 | 62                 | 327                            | 94                   | 19    | 22     |  |
| Asian tower     | 5130       | 1/30 | 47                 | 61                             | 15                   | 6     | 5      |  |
|                 |            | 1/50 | 109                | 219                            | 62                   | 11    | 10     |  |
| Modern building | 2632       | 1/30 | 35                 | 32                             | 16                   | 6     | 7      |  |
|                 |            | 1/50 | 78                 | 171                            | 46                   | 9     | 12     |  |

Complexity represents the number of triangular facets constituting the original models. UWR represents unit-to-whole resolution of the voxel space. Time records the time consumption of the procedures of Model voxelization, Structural part identification, and Volume decomposition. In the Result, Nodes stands for the number of recognized structural parts, and Arcs stands for the number of topological connections between different structural parts.

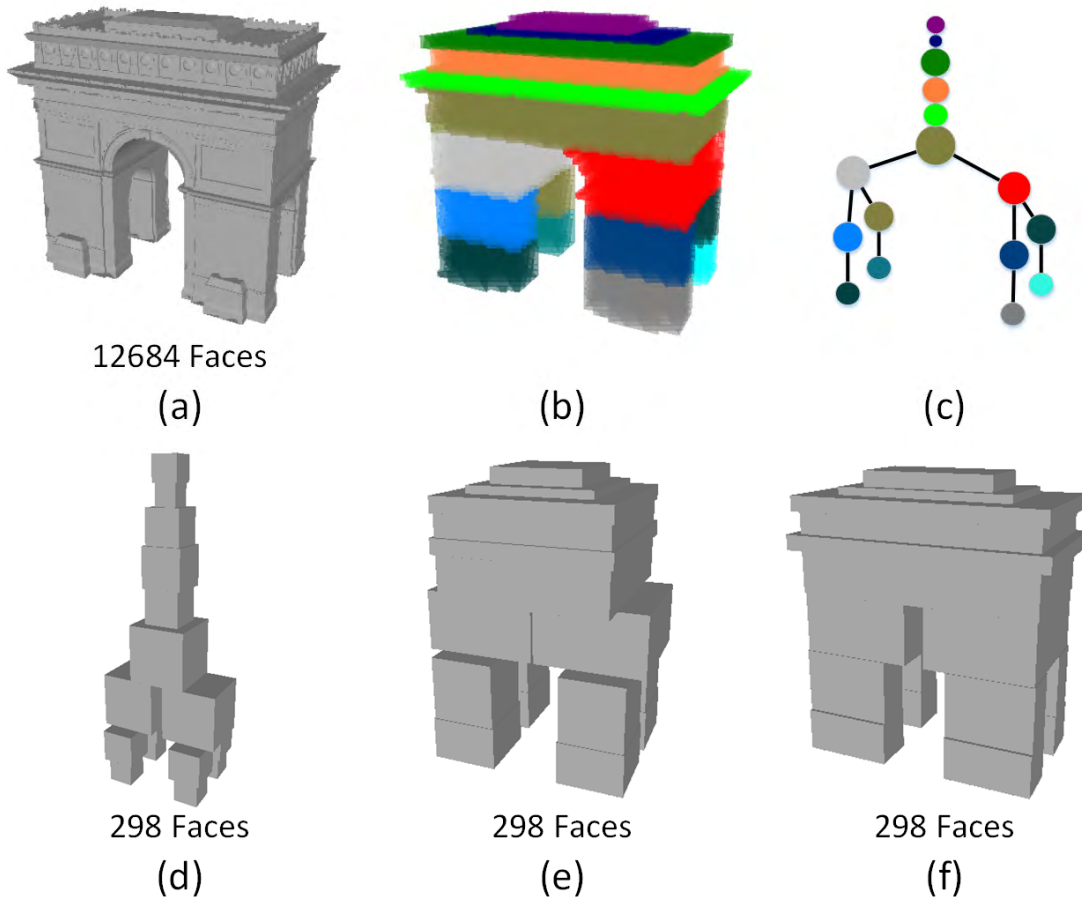
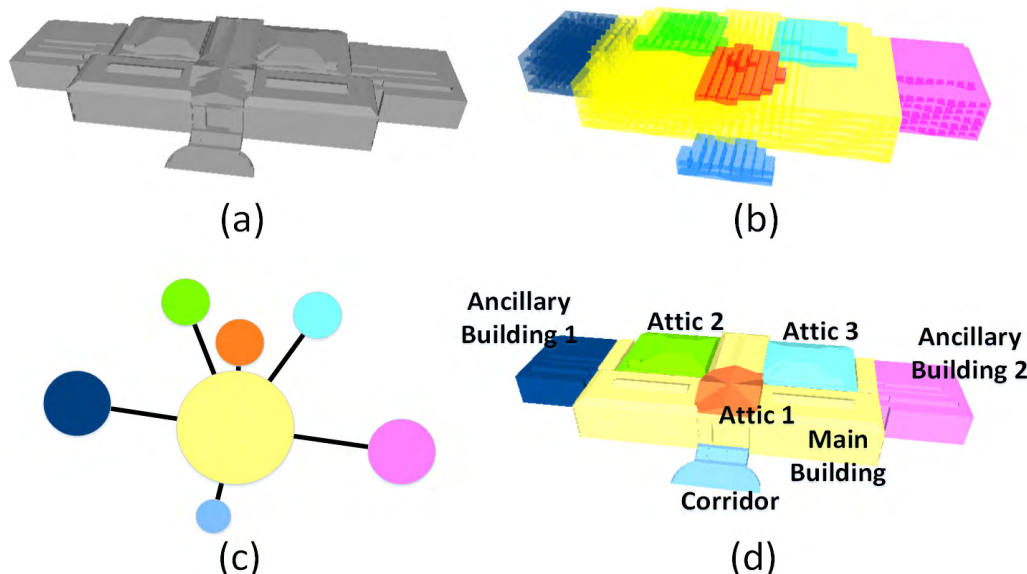


FIGURE 15. Model abstraction based on the structure recognition result. (a) The original building model. (b) Volume decomposition result of the building model. (c) The ETG of the building model. (d) The prototype of the building model obtained through model abstraction, taking advantage of the connection manner attributes of Arcs in the ETG. (e) The abstracted model generated, considering the connection manner attributes of Arcs and approximate heights of Nodes in the ETG. (f) The abstracted model generated, considering the connection manner attributes of Arcs and approximate heights, extension directions and major-minor axis ratios of Nodes in the ETG.

in the voxel space. With the increasing of the discretizing resolution, the fuzziness was able to be reduced and the more accurate descriptions were obtained, which exactly conforms to the variety of the shape recognition depth of human beings on objects. However, the minimum size of the recognized parts was not merely related with the resolution

of the voxel space, but also the specific architectural pattern of the building model. Different shape complexity in the horizontal and vertical directions would result in different granularity of structure recognition under certain resolution.

The experiments were performed using an ordinary laptop with Intel I7-4500U quad-core processors (1.80 GHz),



**FIGURE 16.** Semantic annotation based on the structure recognition result. (a) The original building model. (b) Volume decomposition result of the building model. (c) The ETG of the building model. (d) The semantic model with descriptive information on different parts.

8 GB RAM, and the 64-bit Windows system. The geometric properties of the models, time consumption of each step, and the basic information of the structure recognition results of the experiments are shown in **Tab. 2**.

According to the statistics in **Tab. 2**, the work of structure recognition of any example model was able to be accomplished less than half a second, and the discretizing resolution of the voxel space was definitely the main factor that determined the computation load. By comparison among different models, it is discovered that the geometric complexity (number of triangular facets) of the original building model might only influence the procedure of model voxelization, and the time consumption of the volumetric analysis was actually related with the structure complexity of the model. Taking the models of the European museum and Asian tower for example, although the volume of the latter is about two times that of the former in every resolution, much less time was spent in the procedures of structural part identification and volume decomposition for the latter one. It is because the compositional structure of the Asian tower is obviously simpler than that of the European museum.

**B. EXAMPLE APPLICATIONS**

**1) MODEL ABSTRACTION**

Structure preservation is always a headache for model simplification, especially when the model is abstracted to the version with low level of details [39]. However, based on the ETG produced by our approach, the building model is able to be abstracted to the most simplified versions that keep the basic compositional structure. The more geometric attributes of the Arcs and Nodes in the ETG are considered, the more similar the abstracted model would be with the

original one. For example, providing the connection manner attributes of the arcs, only the prototype of the building model would be obtained; if the approximate heights, extension directions and major-minor axis ratios of nodes are further given, the abstracted model would have less deformation in shape (see **Fig. 15**).

**2) SEMANTIC ANNOTATION**

To satisfy the needs of various high-end applications, such as model documentation [40], digital heritage protection [41], and BIM construction [42], semantic annotation is gaining more and more attention these years. For building models, with reference to the size variation, relative positions and symmetries among different structural parts, a lot of information can be inferred. For example, the main building is always the part lying in the middle or with the maximum size; the ancillary buildings are always connected to the main building or other ancillary buildings side by side in the horizontal direction; the corridors and attics are the small parts in the front or on the top of the whole building model (see **Fig. 16**).

**3) MODEL CLASSIFICATION**

Things of the same category always have similar compositional structure [43], [44]. With the help of the ETGs, it is possible to summarize the structural characteristics of different types of building models and make classification of them based on some distinctive features. For example, the buildings for public services or commercial usage are always composed of a number of departments or sections, so the corresponding 3D models would easily have complex structures in the horizontal and vertical directions; on the

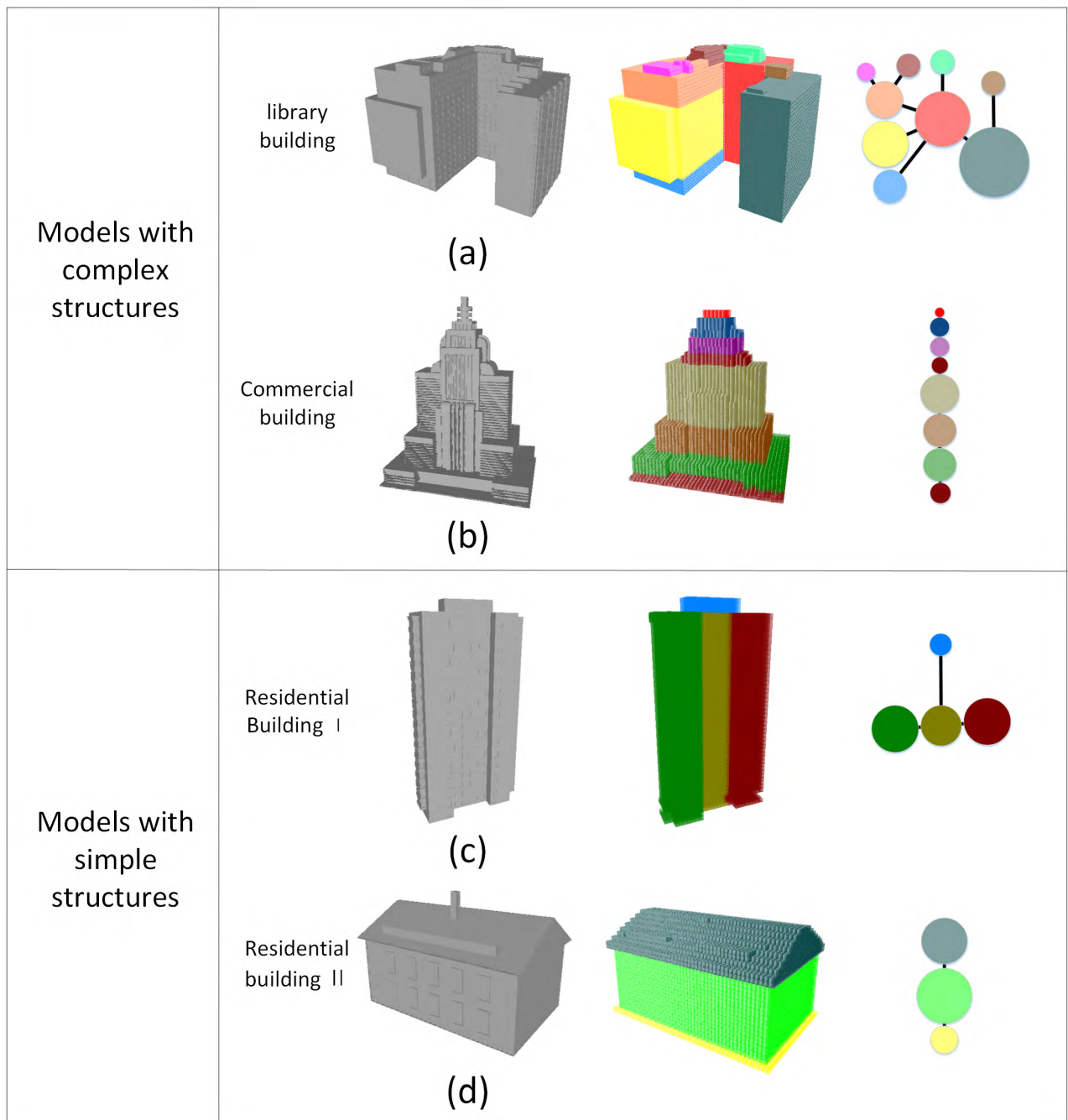


**FIGURE 17.** Building model classification based on the complexity of the compositional structure. (a) The structure description of a library building model. (b) The structure description of a commercial building model. (c) The structure description of a high-rise modern residential building model. (d) The structure description of a low-rise rural residential building model.

contrast, the residential building models generally exhibit simple structures in composition (see Fig. 17).

## VI. CONCLUSION AND OUTLOOK

Compositional structure is a kind of high-level properties of objects. Comparing with the traditional algorithms that are focused on the geometric features on the surfaces, the volumetric analysis provides a new perspective to study the spatial

compositions of 3D building models from inside. Although some noises might be brought in by the procedure of voxelization, the proposed method exhibits great capability in the structure recognition at different scales, not influenced by the construction manner of the surface meshes. Determined by the discretizing resolution of the voxel space, the scale effect of the method well fits in with the various depths and needs of the structure recognition in different applications.

Based on the pioneering work of structure recognition of 3D building models in the voxel space, much more researches and explorations could be carried out in the future. On one aspect, it is possible to extend our approach to other types of man-made object's models and discuss the layered structures of well-designed shapes in the real world. On another aspect, through in-depth studies of the semantic consistency among structural parts obtained under different scales, multi-scale structure recognition in one model might be achieved with some progressive refinement strategies. Moreover, as a supplement to the distance maps adopted in this paper, some other morphological parameters, such as the potential field gradient [45] and symmetry descriptors [46], could also be considered in the process of volumetric analysis to better understand the shapes of the 3D models from different perspectives.

## REFERENCES

- [1] Y. K. A. Tan, L. K. Kwok, and S. H. Ong, "Large scale texture mapping of building facades," *Int. Arch. Photogramm., Remote Sens. Spatial Inf. Sci.*, vol. 37, pp. 687–692, Jul. 2008.
- [2] B. Mao and Y. Ban, "Generalization of 3D building texture using image compression and multiple representation data structure," *ISPRS J. Photogramm. Remote Sens.*, vol. 79, pp. 68–79, May 2013.
- [3] T. Glander and J. Döllner, "Abstract representations for interactive visualization of virtual 3D city models," *Comput., Environ. Urban Syst.*, vol. 33, no. 5, pp. 375–387, Jul. 2009.
- [4] B. Mao, Y. Ban, and L. Harrie, "A multiple representation data structure for dynamic visualisation of generalised 3D city models," *ISPRS J. Photogramm. Remote Sens.*, vol. 66, no. 2, pp. 198–208, Aug. 2011.
- [5] X. Sun, B. Yang, M. Attene, Q. Li, and S. Jiang, "Automated abstraction of building models for 3D navigation on mobile devices," in *Proc. 19th Int. Conf. Geoinf.*, Shanghai, China, Jun. 2011, pp. 1–6.
- [6] J. Zhao, Q. Zhu, Z. Du, T. Feng, and Y. Zhang, "Mathematical morphology-based generalization of complex 3D building models incorporating semantic relationships," *ISPRS J. Photogramm. Remote Sens.*, vol. 68, pp. 95–111, Jan. 2012.
- [7] Q. Zhu and M.-Y. Hu, "Semantics-based 3D dynamic hierarchical house property model," *Int. J. Geograph. Inf. Sci.*, vol. 24, no. 2, pp. 165–188, Feb. 2010.
- [8] G. Gröger and L. Plümer, "CityGML-Interoperable semantic 3D city models," *ISPRS J. Photogramm. Remote Sens.*, vol. 71, pp. 12–33, Jul. 2012.
- [9] Q. Fu, X. Chen, X. Su, J. Li, and H. Fu, "Structure-adaptive shape editing for man-made objects," *Comput. Graph. Forum*, vol. 35, no. 2, pp. 27–36, May 2016.
- [10] M. Kada, "3D building generalization based on half-space modeling," *Int. Arch. Photogramm., Remote Sens. Spatial Inf. Sci.*, vol. 36, pp. 58–64, Feb. 2006.
- [11] F. Thiemann and M. Sester, "Segmentation of buildings for 3D-generalisation," in *Proc. ICA Workshop Gen. Multiple Represent.*, Leicester, U.K., 2004, p. 7.
- [12] Q. Li, X. Sun, B. Yang, and S. Jiang, "Geometric structure simplification of 3D building models," *ISPRS J. Photogramm. Remote Sens.*, vol. 84, pp. 100–113, Oct. 2013.
- [13] G. Vosselman, B. G. H. Gorte, G. Sithole, and T. Rabbani, "Recognising structure in laser scanner point clouds," *Int. Arch. Photogramm., Remote Sens. Spatial Inf. Sci.*, vol. 46, pp. 33–38, Oct. 2004.
- [14] A. Shamir, "A survey on mesh segmentation techniques," *Comput. Graph. Forum*, vol. 27, no. 6, pp. 1539–1556, Sep. 2008.
- [15] X. Chen, A. Golovinskiy, and T. Funkhouser, "A benchmark for 3D mesh segmentation," *ACM Trans. Graph.*, vol. 28, no. 3, p. 73, Jul. 2009.
- [16] M. Garland, A. Willmott, and P. S. Heckbert, "Hierarchical face clustering on polygonal surfaces," in *Proc. Symp. Interact. 3D Graph., Res.*, Triangle Park, NC, USA, 2001, pp. 49–58.
- [17] S. Shlafman, A. Tal, and S. Katz, "Metamorphosis of polyhedral surfaces using decomposition," *Comput. Graph. Forum*, vol. 21, no. 3, pp. 219–228, Sep. 2002.
- [18] G. Lavoue, F. Dupont, and A. Baskurt, "A new CAD mesh segmentation method, based on curvature tensor analysis," *Comput.-Aided Des.*, vol. 37, no. 10, pp. 975–987, Sep. 2005.
- [19] Y. Lee and S. Lee, "Geometric snakes for triangular meshes," *Comput. Graph. Forum*, vol. 21, no. 3, pp. 229–238, Sep. 2002.
- [20] A. F. Koschan, "Perception-based 3D triangle mesh segmentation using fast marching watersheds," in *Proc. IEEE Comput. Soc. Conf. Comput. Vis. Pattern Recognit.*, Madison, WI, USA, Jun. 2003, pp. II-27–II-32.
- [21] D. Marshall, G. Lukacs, and R. Martin, "Robust segmentation of primitives from range data in the presence of geometric degeneracy," *IEEE Trans. Pattern Anal. Mach. Intell.*, vol. 23, no. 3, pp. 304–314, Mar. 2001.
- [22] D. Cohen-Steiner, P. Alliez, and M. Desbrun, "Variational shape approximation," *ACM Trans. Graph.*, vol. 23, no. 3, pp. 905–914, Aug. 2004.
- [23] M. Attene, B. Falcidieno, and M. Spagnuolo, "Hierarchical mesh segmentation based on fitting primitives," *Vis. Comput.*, vol. 22, no. 3, pp. 181–193, Mar. 2006.
- [24] S. Katz, G. Leifman, and A. Tal, "Mesh segmentation using feature point and core extraction," *Vis. Comput.*, vol. 21, nos. 8–10, pp. 649–658, Sep. 2005.
- [25] P. Simari, E. Kalogerakis, and K. Singh, "Folding meshes: Hierarchical mesh segmentation based on planar symmetry," in *Proc. Eurograph. Symp. Geometry Process. (SGP)*, Sardinia, Italy, 2006, pp. 111–119.
- [26] L. Shapira, A. Shamir, and D. Cohen-Or, "Consistent mesh partitioning and skeletonisation using the shape diameter function," *Vis. Comput.*, vol. 24, no. 4, pp. 249–259, 2008.
- [27] R. Guercke, J. Zhaob, C. Brennera, and Q. Zhu, "Generalization of tiled models with curved surfaces using typification," in *Advances in Geo-Spatial Information Science*, W. Shi, M. Goodchild, B. Lees, and Y. Leung, Eds. London, U.K.: Taylor & Francis, 2012, pp. 33–46.
- [28] J.-Y. Rau, L.-C. Chen, F. Tsai, K.-H. Hsiao, and W.-C. Hsu, "LOD generation for 3D polyhedral building model," in *Proc. Pacific-Rim Symp. Image Video Technol.*, Hsinchu, Taiwan, 2006, pp. 44–53.
- [29] R. Mehra, Q. Zhou, J. Long, A. Sheffer, A. Gooch, and N. J. Mitra, "Abstraction of man-made shapes," *ACM Trans. Graph.*, vol. 28, no. 5, p. 137, Dec. 2009.
- [30] K. H. Höhne et al., "3D visualization of tomographic volume data using the generalized voxel model," *Vis. Comput.*, vol. 6, no. 1, pp. 28–36, Jan. 1990.
- [31] D. Cohen-Or and A. Kaufman, "Fundamentals of surface voxelization," *Graph. Models Image Process.*, vol. 57, no. 6, pp. 453–461, Nov. 1995.
- [32] S. Fang and H. Chen, "Hardware accelerated voxelization," *Comput. Graph.*, vol. 24, no. 3, pp. 433–442, Jun. 2000.
- [33] S. W. Wang and A. E. Kaufman, "Volume-sampled 3D modeling," *IEEE Comput. Graph. Appl.*, vol. 14, no. 5, pp. 26–32, Sep. 1994.
- [34] L. Wade and R. E. Parent, "Automated generation of control skeletons for use in animation," *Vis. Comput.*, vol. 18, no. 2, pp. 97–110, 2002.
- [35] J. Wang, Y. He, and H. Tian, "Voxel-based shape analysis and search of mechanical CAD-models," *Forschung Ingenieurwesen*, vol. 71, no. 3, pp. 189–195, Oct. 2007.
- [36] D. D. Hoffman and W. A. Richards, "Parts of recognition," *Cognition*, vol. 18, nos. 1–3, pp. 65–96, 1984.
- [37] D. Hoffman and M. Singh, "Saliency of visual parts," *Cognition*, vol. 63, no. 1, pp. 29–78, Apr. 1997.
- [38] T. Shao, W. Li, K. Zhou, W. Xu, B. Guo, and N. J. Mitra, "Interpreting concept sketches," *ACM Trans. Graph.*, vol. 32, no. 4, pp. 1–10, Jul. 2013.
- [39] M. Garland and P. S. Heckbert, "Surface simplification using quadric error metrics," in *Proc. 25th Annu. Conf. Comput. Graph. Interact. Techn. (ACM SIGGRAPH)*, Los Angeles, CA, USA, 1997, pp. 209–216.
- [40] A. D. Styliadis, "Digital documentation of historical buildings with 3-D modeling functionality," *Autom. Construct.*, vol. 16, no. 4, pp. 498–510, Jul. 2007.
- [41] L. De Luca, C. Busayarath, C. Stefani, P. VèRon, and M. Florenzano, "A semantic-based platform for the digital analysis of architectural heritage," *Comput. Graph.*, vol. 35, no. 2, pp. 227–241, Apr. 2011.
- [42] R. Volk, J. Stengel, and F. Schultmann, "Building information modeling (BIM) for existing buildings—Literature review and future needs," *Autom. Construct.*, vol. 38, pp. 109–127, Mar. 2014.
- [43] M. Ovsjanikov, W. Li, L. Guibas, and N. J. Mitra, "Exploration of continuous variability in collections of 3D shapes," *ACM Trans. Graph.*, vol. 30, no. 4, pp. 1–10, Jul. 2011.
- [44] O. van Kaick et al., "Co-hierarchical analysis of shape structures," *ACM Trans. Graph.*, vol. 32, no. 4, p. 69, Jul. 2013.
- [45] J.-H. Chang, C.-H. Tsai, and M.-C. Ko, "Skeletonisation of three-dimensional object using generalized potential field," *IEEE Trans. Pattern Anal. Mach. Intell.*, vol. 22, no. 11, pp. 1241–1251, Nov. 2000.
- [46] M. Kazhdan, B. Chazelle, D. Dobkin, T. Funkhouser, and S. Rusinkiewicz, "A reflective symmetry descriptor for 3D models," *Algorithmica*, vol. 38, no. 1, pp. 201–225, Jan. 2004.



**XUAN SUN** received the B.S. degree in remote sensing science and technology and the Ph.D. degree in cartography and geographical information engineering from Wuhan University, China, in 2007 and 2013, respectively. He held a post-doctoral position at the University of Glasgow, U.K., in 2017.

From 2005 to 2012, he was the Vice President of the Spacesoft Software Development Association. He is currently the Director of the Digital City Laboratory, Nankai University. He is also hosting the National Scientific Research Foundation Project of China and several open foundation projects sponsored by universities and the Chinese Government. His main research interests comprise urban modeling, urban computing, digital city, and smart city.

Dr. Sun received the second prize of the Public Security Ministry of China for Technical Innovation at Fundamental Departments in 2009, the Excellent Graduated Student of Wuhan University in 2013, and the Innovative Talent of Tianjin in 2015.



**QINGQUAN LI** received the B.S. degree in engineering survey, the M.S. degree, and the Ph.D. degree in photogrammetry and remote sensing from Wuhan University, China, in 1984, 1988, and 1998, respectively.

Since 1998, he has been a Professor with the State Key Laboratory of Information Engineering in Surveying, Mapping and Remote Sensing, Wuhan University. From 2000 to 2012, he was the Vice President of Wuhan University. He is currently the President of Shenzhen University. He is the author of five books and over 400 articles, and holding 13 software copyrights and nine invention patents. His research interests include intelligent traffic systems, urban informatics, and smart city. He is a Chief Editor of the *Journal of Geomatics*, and an Associate Editor of the *Journal Acta Geodaetica et Cartographica Sinica* and *Geomatics and Information Science of Wuhan University*.

Dr. Li is an Academician of the International Eurasian Academy of Sciences, a Chief Scientist of the National Key Basic Research and Development Plan, a Panel Member of the National High Technology Research and Development Program, and a Science and Technology Committee Member of the Education Ministry of China. He is also the Founder and the President of ACM SIGSPATIAL China branch, the President of the International Society for Photogrammetry and Remote Sensing WG II/7, the Vice President of the China Association for Geographic Information System, and the Founder and the President of the Society of GIS-T. He was a recipient of the title National Expert with Remarkable Contributions and National talent of New Century China, and received a Special Allowance from the State Council. He has ever received the second prize of the National Science and Technology Progress, two times of first prize of the Science and Technology Progress of the Ministry of Education, and the first prize in Geographic Information Science and Technology Progress of China.



**BISHENG YANG** received the B.S. degree in engineering survey, the M.S. degree, and the Ph.D. degree in photogrammetry and remote sensing from Wuhan University, China, in 1996, 1999, and 2002, respectively. From 2002 to 2006, he held a post-doctoral position at the University of Zurich, Switzerland.

Since 2007, he has been a Professor with the State Key Laboratory of Information Engineering in Surveying, Mapping and Remote Sensing, Wuhan University, where he is currently the Director of the 3S and Network Communication Laboratory. He has hosted a project of the National High Technology Research and Development Program, a key project of the Ministry of Education, and four National Scientific Research Foundation Project of China. His main research interests comprise 3-D geographic information systems, urban modeling, and digital city. He was a Guest Editor of the *ISPRS Journal of Photogrammetry and Remote Sensing*, and *Computers & Geosciences*.

Dr. Yang was a recipient of the first prize of the International Society for Photogrammetry and Remote Sensing in 2006, the first prize of the Education Ministry of China in 2009, the first prize of Science and Technology Progress of Hubei Province in 2016, and the National Outstanding Youth Fund in 2017. He is a Distinguished Professor of Yangtze River Scholar of the Education Ministry of China and the President of the Point Cloud Treatment Working Group of the International Society for Photogrammetry and Remote Sensing and the Laser Scanning Working Group of the International Association of Geodesy.

•••